



Improved Representation of Agricultural Land Use and Crop Management for Large Scale Hydrological Impact Simulation in Africa using SWAT+

Albert Nkwasa¹, Celray James Chawanda¹, Jonas Jägermeyr^{2,3,4}, Ann van Griensven^{1,5}

5 ¹ Hydrology and Hydraulic Engineering Department, Vrije Universiteit Brussel (VUB), 1050 Brussel, Belgium

² NASA Goddard Institute for Space Studies, New York, NY 10025, USA

³ Center for Climate Systems Research, Columbia University, New York, NY 10025, USA

⁴ Climate Resilience, Potsdam Institute for Climate Impact Research (PIK), Member of the Leibniz Association, 14412, Potsdam, Germany

10 ⁵ Water Science & Engineering Department, IHE Delft Institute for Water Education, 2611 AX Delft, The Netherlands

Correspondence to: Albert Nkwasa (albert.nkwasa@vub.be)

Abstract. To date, most regional and global hydrological models either ignore the representation of cropland or consider crop cultivation in a simplistic way or in abstract terms without any management practices. Yet, the water balance of cultivated areas is strongly influenced by applied management practices (e.g. planting, irrigation, fertilization, harvesting). The SWAT+ model represents agricultural land by default in a generic way where the start of the cropping season is driven by accumulated heat units. However, this approach does not work for tropical and sub-tropical regions such as the sub-Saharan Africa, where crop growth dynamics are mainly controlled by rainfall rather than temperature. In this study, we present an approach on how to incorporate crop phenology using decision tables and global datasets of rainfed and irrigated croplands with the associated cropping calendar and fertilizer applications in a regional SWAT+ model for Northeast Africa.

15 We evaluate the influence of the crop phenology representation on simulations of Leaf Area Index (LAI) and Evapotranspiration (ET) using LAI remote sensing data from Copernicus Global Land Service (CGLS) and WaPOR ET data respectively. Results show that a representation of crop phenology using global datasets leads to improved temporal patterns of LAI and ET simulations, especially for regions with a single cropping cycle. However, for regions with multiple cropping seasons, global phenology datasets need to be complemented with local data or remote sensing data to capture additional cropping seasons. In addition, the improvement of the cropping season also helps improve soil erosion estimates, as the timing of crop cover controls erosion rates in the model. With more realistic growing seasons, soil erosion is largely reduced for most agricultural Hydrologic Response Units (HRUs) which can be considered as a move towards substantial improvements over previous estimates. We conclude that regional and global hydrological models can benefit from improved representations of crop phenology and the associated management practices. Future work regarding incorporating multiple cropping seasons in global phenology data is needed to better represent cropping cycles in regional to global hydrological models.

20
25
30



1 Introduction

Even though cropland cultivation covers over 40 % of the planet's ice-free land surface, most regional and global hydrological models either ignore the representation of cropland or consider crop cultivation in a simplistic way or in abstract terms without any management practices (Sood and Smakhtin, 2015; Srivastava et al., 2020). In most cases, the models neither address crop phenological development nor distinguish between different crops and the associated management practices (e.g. planting, irrigation, fertilization, harvesting) (Chen and Xie, 2012; Srivastava et al., 2020). Yet, the water balance of cultivated areas is strongly influenced by applied management practices and their precise timing (Twine et al., 2004). In the context of global change studies, realistic representation of agricultural systems is a major concern as changes in climatic factors affect crop growth and productivity of agricultural systems (Makowski et al., 2014). Therefore, hydrological models that simulate cropland ecosystems should have a reasonable representation of crop phenology and the associated management practices of these ecosystems (Lokupitiya et al., 2009).

The SWAT+ model (Bieger et al., 2017; Arnold et al., 2018) which is a restructured version of SWAT (Soil and Water Assessment Tool; Arnold et al., 1998) utilizes the principles of the EPIC crop growth model (Williams and Singh, 1995) to simulate agricultural land by default in a generic way where the phenological development of crops from planting is driven by accumulated heat units (Arnold et al., 1998). However, the primary controlling factor for the start of the growing season in tropical and sub-tropical regions such as the sub-Saharan Africa is rainfall (Lotsch et al., 2003; Alemayehu et al., 2017). Waha et al., (2013) describes the crop growing season in sub-Saharan Africa as the period in which temperature and moisture are suitable for growth determined by the start and end of the main rainy season. Zhang et al., (2005) showed that the onset of seasonal vegetation green-up across Africa can be directly linked to rainfall seasonality. Studies (e.g. Msigwa et al., 2019, Nkwasa et al., 2020) have further pointed out how the existing multiple cropping seasons in tropical and subtropical climates within an agricultural year coincide with the rainfall and irrigation patterns. Therefore, the use of heat units to trigger the start of the cropping seasons could lead to inconsistencies in crop phenology simulations for tropical and sub-tropical regions.

Croplands include various types with associated differences in crop physiology and management practices (Lokupitiya et al., 2009; Yin and Struik, 2009). The phenological change during the vegetation cycle of crop types actively controls the ET process through internal physiology by increasing the amount of leaf stomata with canopy growth (Gong et al., 2014). In the SWAT+ model, plant transpiration is simulated as a linear function of Leaf Area Index (LAI) and Potential Evapotranspiration (PET) (Neitsch et al., 2005). Thus, inconsistencies in crop simulations could lead to inaccurately estimating canopy properties such as LAI and canopy height resulting in uncertain estimates of ET (Alemayehu et al., 2016). Accurate estimations of ET in a hydrological model are important because ET is the central flux that defines land-atmosphere interactions (Mueller et al., 2011; Fisher et al., 2017).

Additionally, changes in cropland use and crop management have received little attention in hydrological impact assessments yet these may have more significant impacts on model outputs such as soil erosion and sediment yield than rainfall and temperature (O'Neal et al., 2005). Abaci and Papanicolaou, (2009) further stated that cropland management practices can



65 significantly affect the impact of precipitation on soil erosion. Cropland practices cause great variations in the erodibility of
cropland since soil erosion depends on what crop is grown and the crop cover density (Sundborg and White, 1982). The crop
cover is crucial in the estimation of the C (crop management) factor in erosion models such as the Modified Universal Soil
Loss Equation (MUSLE) used by SWAT+ (Lin et al., 2014). Other crop management practices such as amounts of fertilizer,
alters soil ability to produce biomass and thus alters soil resistance to erosion (Souza et al., 2017). The timing and duration of
70 soil cover on cropland are affected by the planting and maturity dates of the crop.

Previous studies have applied the SWAT model at a regional scale within and including sub-Saharan Africa (Schuol and
Abbaspour, 2006; Schuol et al., 2008). However, these studies utilized the default generic way of representing agricultural
land use without any management practices. Yet, Arnold et al., (2012) emphasized the need for realistic representation of local
and regional crop processes to reliably simulate the water balance, erosion and nutrient yields in a SWAT model. One wonders
75 whether these regional studies consider an accurate representation of the internal catchment processes of crop phenology and
vegetation dynamics. Chawanda et al., (2020) describes one of the few regional applications of the latest SWAT+ version in a
tropical region. The study highlighted that the inclusion of irrigation and reservoirs in model set up using decision tables
(Arnold et al., 2018) led to an improvement on the simulations of discharge and ET.

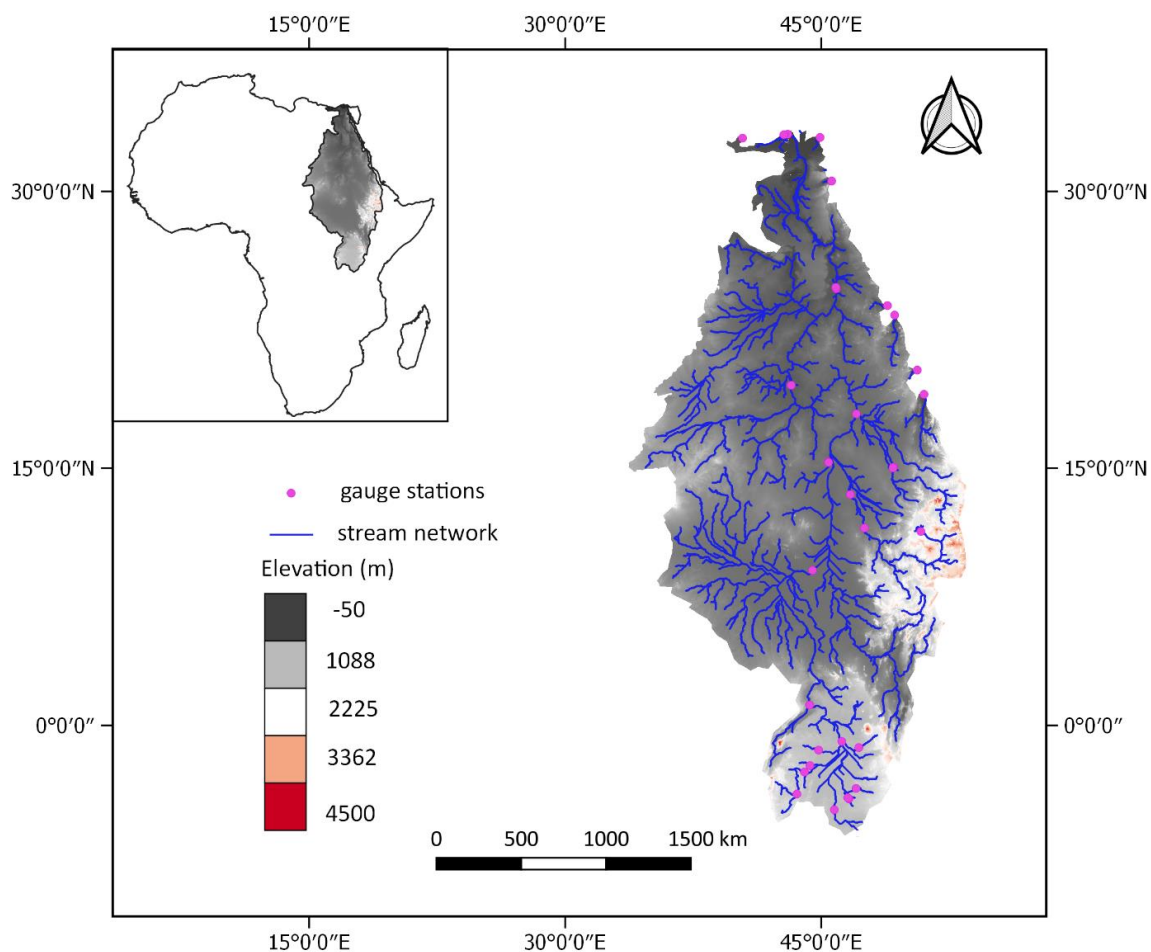
Regional cropping phenology datasets and management practices have been developed using remote sensing approaches (Li
80 et al., 2014; Estel et al., 2016; Xiong et al., 2017) and non-remote sensing approaches, including observational census data
(Potter et al., 2010; Portmann et al., 2010; Lu and Tian, 2017; Iizumi et al., 2019; Hurtt et al., 2020; Jägermeyr et al., in
revision), to integrate into regional agricultural and hydrologic modelling frameworks. However, remote sensing approaches
have been criticized as not being able to detect crop types and cropping sequences without local knowledge or ground truth
data (Bégué et al., 2018). Nevertheless, these spatially explicit global cropping phenology data sets have not been utilized in
85 regional hydrological models to improve the land use and crop representation.

The novelty of this study is in improving land use and crop process representation for large scale hydrological modelling using
SWAT+ by (1) proposing an approach that reasonably incorporates crop phenology using decision tables and global datasets
of rainfed and irrigated croplands with the associated management practices in a regional SWAT+ model for Northeast Africa,
(2) evaluating model improvements of crop representation by using the remote sensing LAI from Copernicus Global Land
90 Service (CGLS) and ET derived from WaPOR (Water Productivity through Open access of Remotely sensed derived data,
FAO, 2018), (3) evaluating how the consideration of crop phenology and the associated management practices affects long
term water-driven soil erosion estimates. We do not intend to fully model soil erosion but show how improvements in crop
representation can impact soil erosion estimates.

2 Material and Methods

2.1 Study area

Our study area in Figure 1 is the North-eastern part of Africa that covers 4,489,000 km². This area includes wholly or partially countries of the Nile basin including Uganda, Kenya, Tanzania, Rwanda, Burundi, Sudan, South Sudan, Ethiopia, Egypt. The area includes the main Nile basin with sub basins such as, Victoria Nile, Blue Nile, White Nile, Atbara, Baro-Akobo-Sobat, Bahr El jebel and Bahr El Ghazal. The agricultural sector is responsible for nearly 75 % of the water withdraw within the basins (Swain, 2011). A strong latitudinal wetness gradient characterizes the climate of the region. The areas north of 18°N remain dry mostly of the year while there is a gradual increase of monsoon precipitation amounts in the south (Camberlin, 2009).



105

Figure 1: Study area - Northeast Africa (Nile basin)



2.2 Modelling approach using SWAT+

SWAT+ is a revised version of SWAT that offers greater flexibility in connecting spatial units in the representation of management operations (Bieger et al., 2017; Arnold et al., 2018). This is a semi-distributed river basin scale model that relies on the physical characteristics of a catchment. It divides a basin into sub basins connected by a stream network, which are further divided into Hydrologic Response Units (HRUs). HRUs represent areas within the sub basin that comprise of the same land use, soil, slope and management practices (Neitsch et al., 2005). SWAT+ also introduces landscape units (LSU) to allow separation of lowland (wetland) processes from upland process (Bieger et al., 2017). SWAT+ applies the hydrological water balance concept, Eq. (1) as the basic driver of all hydrological processes.

$$WB_f = WB_i + \sum(P_j - R_j - E_j - D_j - RF_j) * \Delta t \quad (1)$$

Where; WB_f and WB_i are the final and initial soil water content respectively (mm d^{-1}), P_j is the amount of rainfall (mm d^{-1}), R_j is the amount of surface runoff (mm d^{-1}), E_j is the ET amount (mm d^{-1}), D_j is the percolation amount (mm d^{-1}), RF_j is the return flow amount (mm d^{-1}), Δt is the change in time (day) and j is the index. The model estimates erosion and sediment yield for each HRU using the Modified Universal Soil Loss Equation (MUSLE) (Williams and Berndt, 1977), Eq. (2). The MUSLE uses runoff energy rather than rainfall to estimate sediment yields, making it suitable at daily time scale.

$$Sed = 11.8 (Q_{surf} q_{peak} Area_{hru})^{0.56} \times K_{USLE} \times C_{USLE} \times P_{USLE} \times LS_{USLE} \times CFRG \quad (2)$$

where; Sed is the sediment yield (tonnes/day), Q_{surf} is the surface runoff volume (mm/day), q_{peak} is the peak runoff rate (m^3/s), $Area_{hru}$ is the area of the HRU (ha), K_{USLE} is the USLE soil erodibility factor, C_{USLE} is the USLE crop management factor, P_{USLE} is the USLE support practice factor, LS_{USLE} is the USLE topographic factor and CFRG is the coarse fragment factor.

Land use and management operations in SWAT+ can be scheduled using either or both decision tables and management schedules. However, decision tables enable the user to model intricate sets of rules and their subsequent actions by allowing them to add conditions for scheduling management (Arnold et al., 2018). Nkwasa et al., (2020) compared the use of decision tables to management schedules and concluded that decision tables provided higher flexibility in representing agricultural practices.

2.3 Crop growth cycle with heat unit scheduling

SWAT+ uses the simplified version of the EPIC growth model to simulate plant growth (Neitsch et al., 2005). As in the EPIC model, phenological plant development is based on the daily accumulated heat units or by calendar dates, while plant growth can be inhibited by temperature, water, nitrogen and phosphorus nutrients (Neitsch et al., 2005; Arnold et al., 2012). The heat unit theory assumes that plants have requirements that can be quantified and linked to maturity. The total number of heat units required by the plant to start growing or to reach maturity is calculated as in Eq. (2).

$$PHU = \sum_{d=1}^n (T_{av} - T_{base}) \text{ when } T_{av} > T_{base} \quad (2)$$

where; PHU is the total heat units required to plant maturity, T_{av} is the mean daily temperature ($^{\circ}\text{C}$), T_{base} is the plant's minimum temperature for growth ($^{\circ}\text{C}$), $d = 1$ is the day of planting and n is the number of days required for a plant to reach



maturity. Planting is scheduled by a second heat index where heat units are summed over the entire year using $T_{base} = 0^{\circ}\text{C}$.
140 This heat index is solely a function of climate calculated by SWAT+ using the provided long-term weather data (Neitsch et al., 2005).

While scheduling by heat units is convenient for temperate regions that are mainly driven by temperature, users need to consider that cropping seasons in tropical and sub-tropical regions are primarily driven by water availability (Alemayehu et al., 2017). Hence, the use of heat units causes incorrect cropping seasons for these regions.

145 **2.4 Default Model set up**

The SWAT+ model was set up with the QGIS interface using the data in Table 1. An approach suggested by Chawanda et al., (2020) was used in the model set up since the state-of-the-knowledge harmonized land use product that is formatted in NetCDF was adapted in this study. By default, the cropland was represented in a generic way using heat units to trigger the cropping seasons. The study area was discretized into 768 landscape units and 12526 unsplit HRUs. The USDA Soil
150 Conservation Service (SCS) curve number method was used to estimate surface runoff, variable storage method selected for flow routing and the Penman-Monteith method (Monteith, 1965) used to calculate the potential evapotranspiration.

Table 1: Global datasets used for model setup and crop management

| Global Datasets | Resolution | Source |
|-------------------------------|-------------------------|--|
| Digital Elevation Model (DEM) | 90 m resampled to 250 m | Shutter Radar Topography Mission (SRTM; Farr et al., 2007) |
| Land use | 0.25° | Harmonized land use (LUH2; Hurtt et al., 2020) |
| Soil | 250 m | Africa Soil information Service (AFSIS; Hengl et al., 2015) |
| Climate | 0.5° | Earth2Observe, WFDEI and ERA-Interim data Merged and Bias corrected for ISIMIP (EWEMBI; Lange, 2016) |
| Irrigated areas | 0.083° | Food and Agriculture Organization (FAO; Siebert et al., 2013) |
| Plant and harvest dates | 0.5° | Global Gridded Crop Model Intercomparison (GGCMI; Jägermeyr et al., in revision) |
| Fertilizer – Nitrogen(N) | 0.5° | (Hurtt et al., 2020) |
| Fertilizer – Phosphorus(P) | 0.5° | (Lu and Tian, 2017) |

2.5 Proposed scheduling - Crop growth cycle with global phenology datasets

The land use map (LUH2; Hurtt et al., 2020) is a composite of land use layers with each layer representing a fraction of a given
155 land use. The fraction layers representing cropland include; C3 annual crops (C3ann), C3 perennial crops (C3per), C4 annual crops (C4ann), C4 perennial crops (C4per) and C3 nitrogen-fixing crops (C3nfx). These layers were extracted and comparison

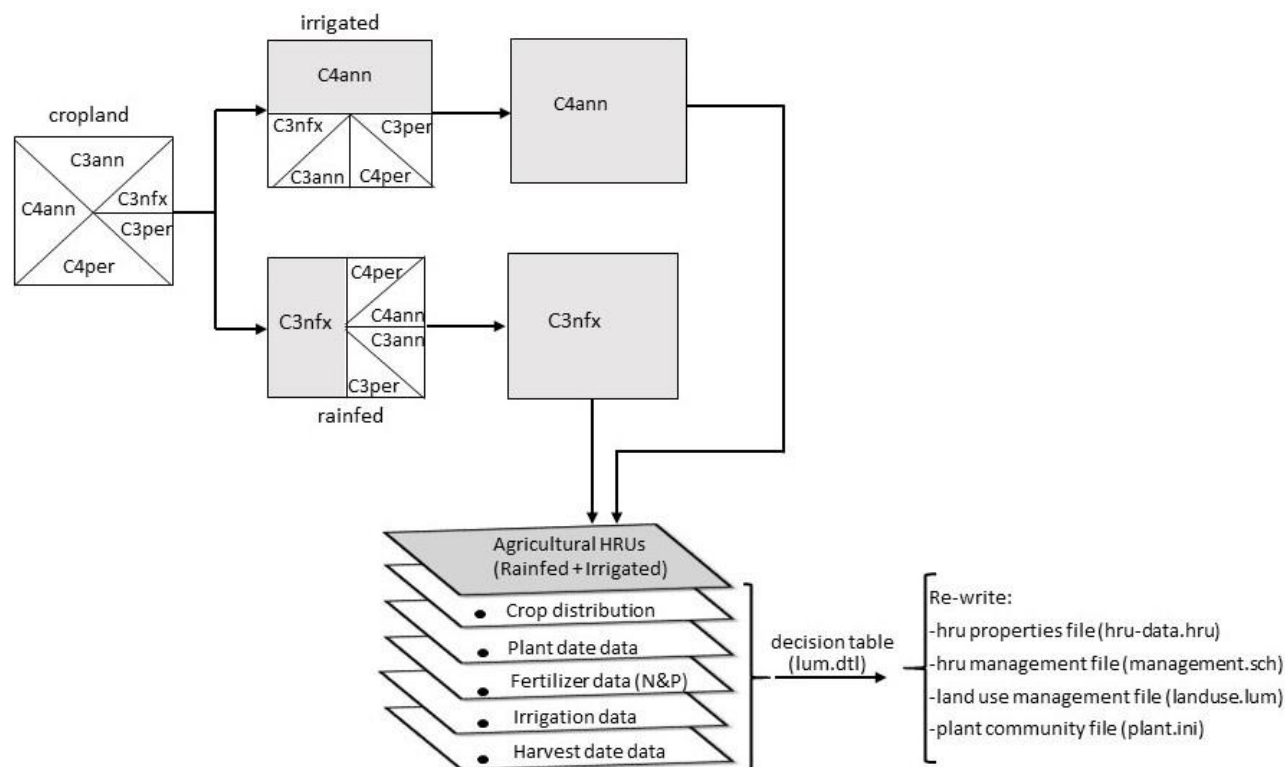


was made on a pixel by pixel basis. Whatever crop layer fraction occupied a larger percentage for the rainfed and irrigated agricultural areas within a pixel was selected to represent cropland for irrigated and rainfed areas in that pixel. For example in Figure 2; if the C4ann and C3nfx crop occupied a larger fraction within a pixel compared to other cropland use fraction layers for irrigated and rainfed cropland respectively, they were selected to represent cropland use in that pixel. A crop map was developed from this pixel by pixel analysis and a representative crop selected for each cropland use fraction based on literature (Leff et al., 2004) as shown in Table 2.

Table 2: Representative crop for LUH2 cropland used in SWAT+

| cropland (LUH2) | Representative crop (SWAT+) |
|--------------------|-----------------------------|
| C3 annual | wheat |
| C3 perennial | banana |
| C4 annual | maize |
| C4 perennial | sugarcane |
| C3 nitrogen-fixing | soybean |

For both rainfed and irrigated areas, the representative crops with the corresponding crop phenology (plant and harvest dates) and crop management practices (irrigation, N-fertilizer and P-fertilizer) were extracted from the respective global datasets (Table 1). The extracted data was written in a decision table for each cropland HRU using a python code. The default model was re-run with the modified crop scheduling with data from global datasets and referred to as ‘revised SWAT+’ model from here on.



170 **Figure 2:** Workflow for incorporating crop phenology and crop management data from global datasets into the model

2.6 Validation of model results

Our study focused on improved cropland use representation. We evaluated our simulations for LAI and ET for a period of 7 years (2009 – 2015) using remote sensing products from CGLS (<https://land.copernicus.vgt.vito.be/>) and WaPOR respectively. Studies (e.g., Alemayehu et al., 2017; Ha et al., 2018; Nkwasa et al., 2020) have demonstrated the capability of using remote

175 sensing products to evaluate hydrological model outputs. Representative basins in the model as shown in Figure 3 were selected to highlight the importance of incorporating global phenology datasets on LAI simulations in regional hydrological modelling. The selected basins were based on the reported cropping patterns that start with the rainy season (Waha et al., 2013) i.e Upper Blue Nile basin with a predominantly single cropping season, Victoria basin with a double cropping season and the Nile delta with mainly a double irrigated cropping season (Sugita et al., 2017; M. El-Marsafawy et al., 2018). Crop HRUs within the

180 selected sub-basins, that occupied the largest areas were selected to reduce the effect of mixed LAI from different land cover classes when comparing with the remote sensing LAI.

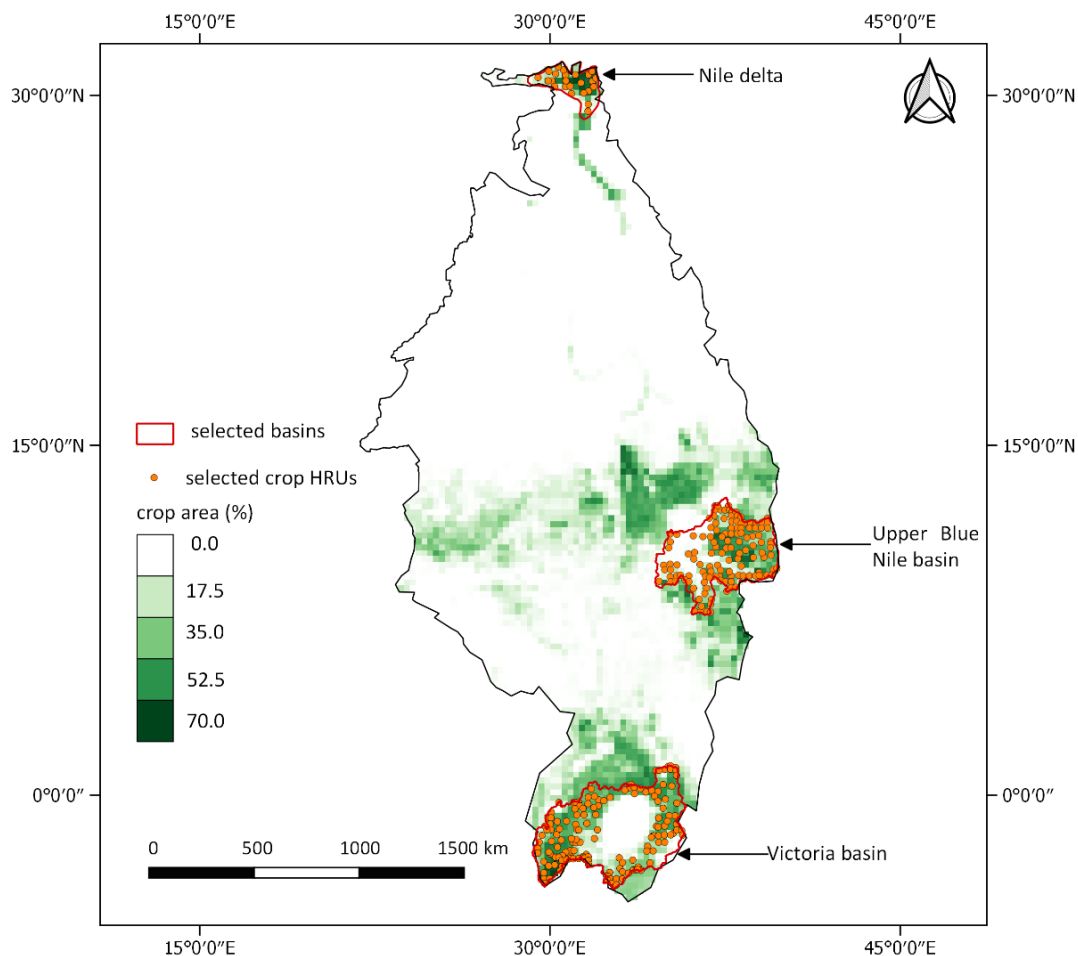


Figure 3: Crop area percentage and selected basins for LAI evaluation

Additionally, the correlation coefficient matrix, Eq. (3) was used for model evaluation of LAI.

$$185 \quad r = \frac{\sum_{i=1}^n (Y_{m_i} - \bar{Y}_m)(Y_{o_i} - \bar{Y}_o)}{\sqrt{\sum_{i=1}^n (Y_{m_i} - \bar{Y}_m)^2} \sqrt{\sum_{i=1}^n (Y_{o_i} - \bar{Y}_o)^2}} \quad (3)$$

where; Where; Y_{m_i} and Y_{o_i} are the simulated and observed values at every time step, with \bar{Y}_m and \bar{Y}_o being the respective mean values.

To illustrate the impact of revised cropland use representation on model outputs, we compare the differences in soil erosion simulations between the default and the revised SWAT+ models. However, due to the sparse and poor quality records of erosion and sediment yield in this region (Haregeweyn et al., 2017), it was not possible to quantitatively validate erosion model results. Instead, we adopted a ‘scientific validation’ approach that is suitable for cases when observations for comparison with model outputs are limited and when the model is utilized to advance the knowledge of physical processes (Biondi et al., 2012). We compared our erosion estimates for some catchments e.g. Upper Nile with those from a few previous studies (Hurni,



195 1985; Betrie et al., 2011; Haregeweyn et al., 2017). Moreover, the improvement in the representation of crop phenology and
crop management practices was intended to minimize errors associated with estimating soil erosion, specifically the crop
management factor in the MUSLE.

Both model setups were uncalibrated but checked for the water balance because even with the best possible model calibration
for both model setups, model discrepancies due to crop representation could not have been isolated. This approach could not
only isolate the uncertainty in the model due to crop representation but also allow the model results be compared in default
200 parameter conditions, considering parameter calibrations vary with different catchments. Nkwasa et al., (2020) also suggested
that improved representation of crop and agricultural land use processes should precede any model calibration efforts. Besides,
SWAT was developed with the objective of predicting the impact of management on water, sediment and agricultural yields
in large ‘ungauged’ basins (Arnold et al., 1998; Srinivasan et al., 2010).

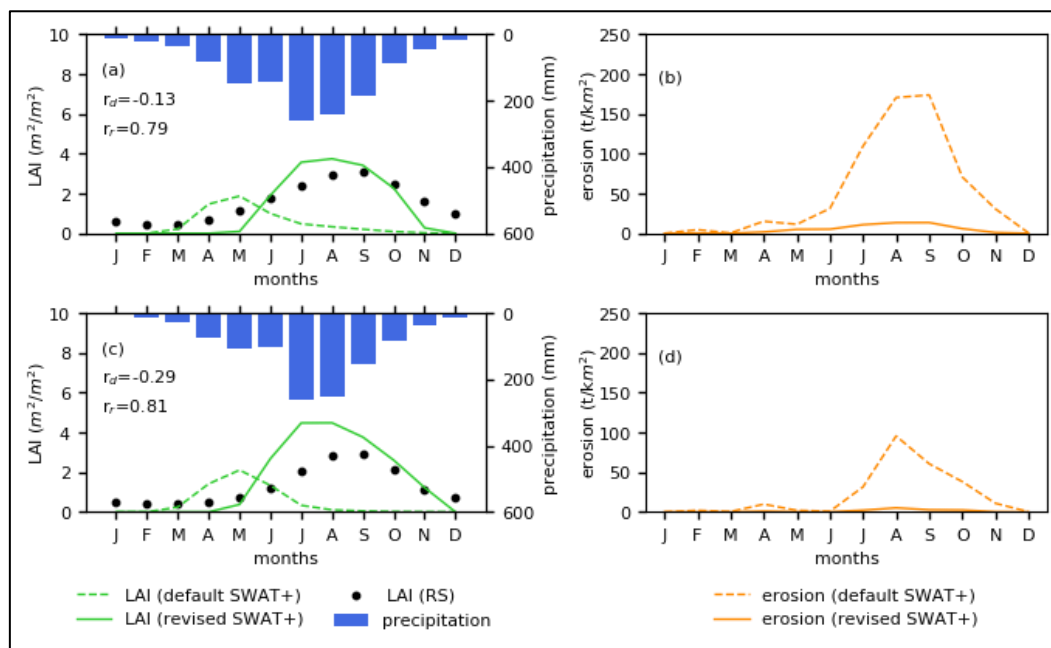
In addition, the uncalibrated models already had good water balance estimates (0.5% and 0.4% for the default and revised
205 models respectively) calculated using Eq. (1) for the simulated period. We assume that the differences seen in the model setups
originate primarily from the crop representation and management practices. Hence, we do not address issues concerning the
SWAT+ model calibration and validation in this paper.

3. Results and discussion

3.1 LAI simulations

210 The simulated LAI from both the default and revised SWAT+ models was compared with the remote sensing LAI extracted
for the maize, wheat and soy HRUs in the 3 selected sub-basins (Upper Blue Nile, Lake Victoria and Nile Delta). In the Upper
Blue basin, Figure 4(a) and Figure 4(c), there is an improved LAI simulation in the revised SWAT+ model with the
phenological development being captured in the correct major cropping season within the rainy season for both the rainfed and
irrigated maize HRUs. Additionally, the revised SWAT+ model LAI strongly correlates ($r_d > 0.5$) with the remote sensing
215 (RS) LAI. Figure A1(a) and Figure A1(c) in the Appendix A, also shows the improvement in LAI simulations for rainfed and
irrigated wheat HRUs in the Upper blue Nile basin.

In the Victoria basin, (Figure 5(a) and Figure 5(c)), the revised SWAT+ model captures only one cropping season in
comparison to the RS LAI that shows a double seasonal pattern agreeing with the rainfall. This is because the global data set
utilized captures only the main cropping season per pixel per crop and hence the model misses the additional cropping seasons
220 (Jägermeyr et al., in revision).



225 **Figure 4:** (a) LAI comparison for rainfed maize, (b) Erosion estimates for rainfed maize, (c) LAI comparison for irrigated maize (d) Erosion estimates for irrigated maize in the Upper Blue Nile basin. The LAI correlation coefficients (r_d for the default SWAT+ model and r_r for the revised SWAT+ model)

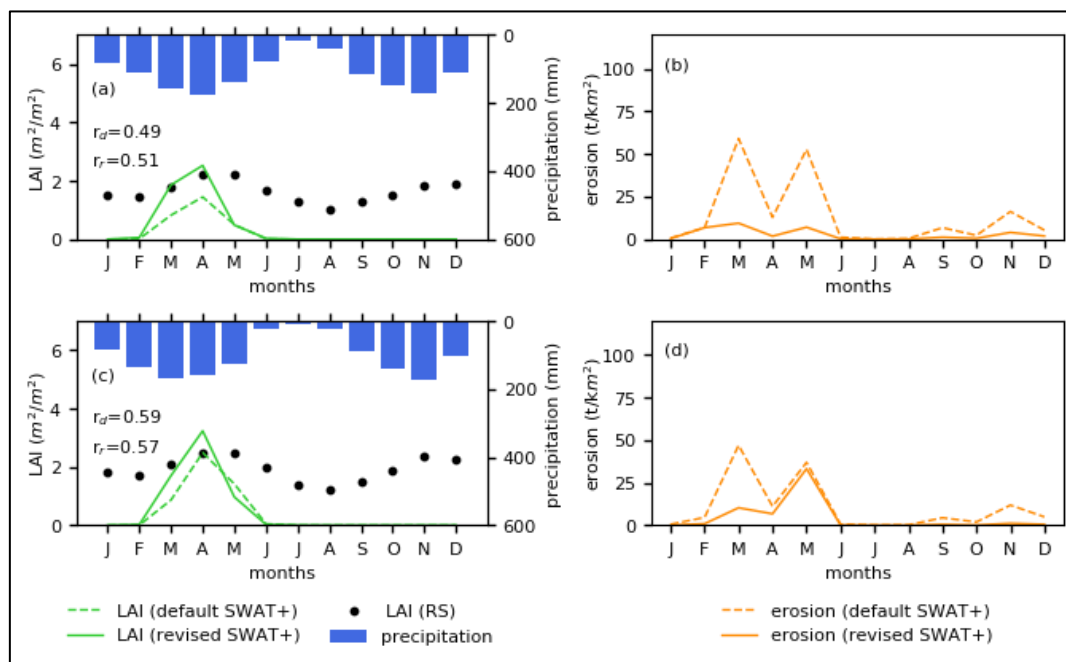
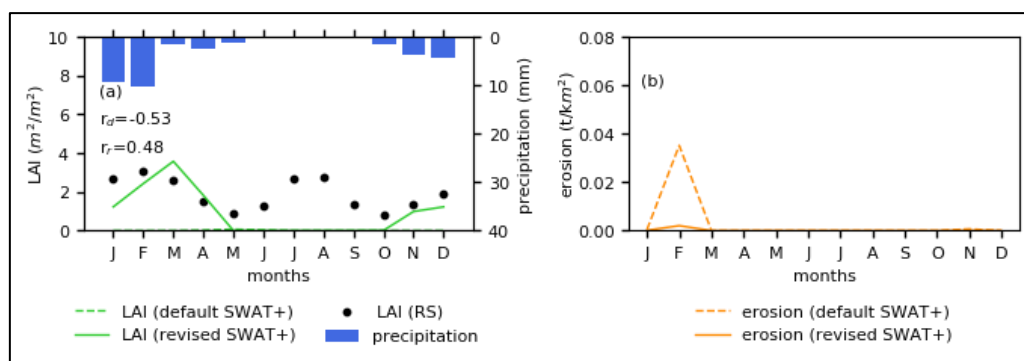


Figure 5: (a) LAI comparison for rainfed wheat, (b) Erosion estimates for rainfed wheat, (c) LAI comparison for irrigated wheat (d) Erosion estimates for irrigated wheat in the Victoria basin. The LAI correlation coefficients (r_d for the default SWAT+ model and r_r for the revised SWAT+ model)



- 230 Additionally, Figure A2(a) and Figure A2(c) in the Appendix A also show a single cropping season captured in the Victoria basin for irrigated maize HRUs with some HRUs having a cropping season from April to November while others have a cropping season from September to January. There is also a slight improvement in the LAI correlations for the default and revised SWAT+ models with RS LAI in the Victoria basin as the LAI simulated by the revised SWAT+ model are indicative of the representative crops planted in the basin as compared the generalized crop representation in the default model.
- 235 For the Nile delta that is predominantly irrigated, the revised SWAT+ model improves the LAI simulations (from $r_d = -0.53$ to 0.48) as compared to the default SWAT+ model that simulates a negligible LAI, Figure 6(a). However, it still captures only one cropping season as compared to the RS LAI that shows two cropping seasons that are also highlighted in previous studies (M. El-Marsafawy et al., 2018).



- 240 **Figure 6:** (a) LAI comparison for irrigated wheat, (b) Erosion estimates for irrigated wheat in the Nile delta. The LAI correlation coefficients (r_d for the default SWAT+ model and r_r for the revised SWAT+ model)

- From all the basins, we see an improved seasonal temporal crop-growth phenological development pattern with the revised model as compared to the default model for both the rainfed and irrigated regions. However, in the Victoria basin and the Nile delta where we have two dominant cropping seasons, the global datasets still capture one cropping season. Additionally, some regions in East Africa have been reported to have up to 3 cropping seasons (Waha et al., 2013; Msigwa et al., 2019) which causes some errors in the model outputs. The global crop calendars also lack a temporal time series dimension which could be a substantial source of uncertainties in predicting phenological events of croplands. Another source of uncertainties could be the use of remote sensing LAI data (1km resolution) in evaluation that does not represent a pure signal of a crop but rather vegetation with in the pixel. Nkwasa et al., (2020) highlighted these scaling issues when using remote sensing products in model evaluation. Nevertheless, the remote sensing data still provides insights on the temporal vegetation growth relationship with seasonal weather patterns.

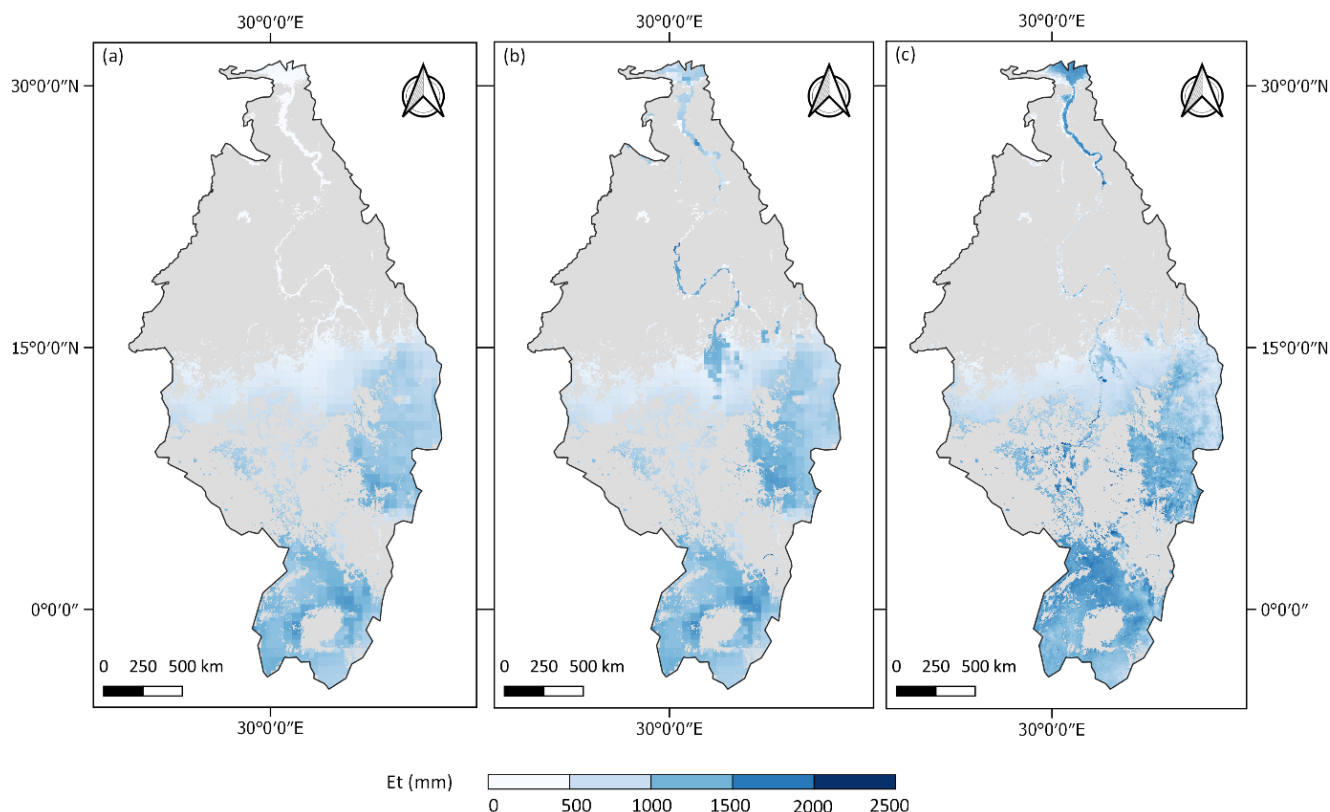
3.2 ET simulations

The annual average simulated agricultural ET from the revised SWAT+ model improves the default agricultural ET simulation from 732 mm y⁻¹ to 837 mm y⁻¹ as compared to the WaPOR agricultural ET of 936 mm y⁻¹. Figure 7 shows the improvement



255 in the spatial distribution of the agricultural ET with the revised SWAT+ model, Figure 7(b) as compared to the default model, Figure 7(a).

The inclusion of the global phenology and management practices shows that ET is one of the major components of a basin water balance that is greatly influenced by the seasonal vegetation growth cycles. Although, the agricultural ET is improved with the incorporation of the global crop phenology, there is still an underestimation. This underestimation could be attributed to the missing multiple cropping seasons especially in areas that are irrigated. Additionally, automatic irrigation was specified in the model which applies water from an unlimited source to the field when the water stress is below a specified threshold (0.7) of the field capacity. However, this may be unrealistic in all irrigation sites causing uncertainties in irrigation applications which affects the ET estimates. Nevertheless, the ET estimates could be further improved by model calibrations to obtain the optimal possible ET.



265

Figure 7: Spatial distribution of agricultural ET; a) default SWAT+ model ET, b) revised SWAT+ model ET, c) WaPOR ET

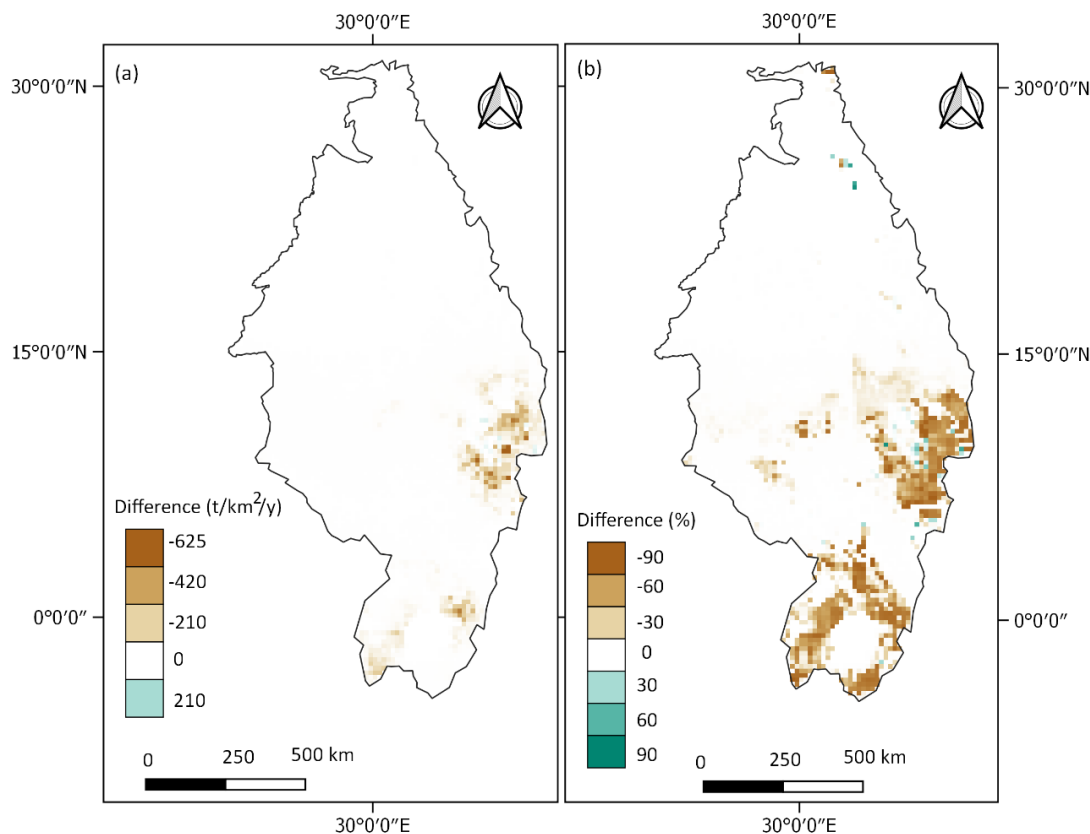
3.3 Erosion simulations

LAI is not only directly related to processes such as rainfall interception, evaporation, transpiration, soil evaporation, root depth but also to soil erosion through canopy cover which varies during the growth cycle of the plant. With a better



270 representation of the cropping season, the rainfall season also corresponds with higher LAI values which results in lower erosion yields.

Figures; 4(b), 4(d), 1A(b), A2(b), A3(d), 4A(b) and A4(d), reveal that the soil erosion estimates are reduced in the revised SWAT+ model because the canopy cover grows in the correct cropping season (rainy season) reducing the effective energy of intercepted raindrops. However, in Figure 5(b) and Figure 5(d), even though the cropping season in the revised SWAT+ model captures only one cropping season as the default model, there is still a reduction in the HRU erosion estimates because the revised SWAT+ LAI, representative of an actual crop is greater than the default LAI representative of a generic crop. Additionally, with more biomass, more residue is generated which could be more effective in reducing soil erosion even after the cropping season. Residue intercepts rain droplets near the soil surface that drops regain no fall velocity (Neitsch et al., 2011). For the Nile delta in Figure 6(b), the soil erosion estimates reduced further even though they were already insignificant. 275 The soil erosion estimates are reduced by a maximum of $625 \text{ t km}^{-2} \text{ y}^{-1}$, Figure 8(a) or up to 90 %, Figure 8(b) in some areas within the region when using the revised SWAT+ model as compared to the default model. The average regional soil erosion yield reduced by 16 %. This reduction is attributed to the improved timing of the cropping seasons in correspondence to the start of the rainy season which provides more canopy cover to intercept the raindrops. 280



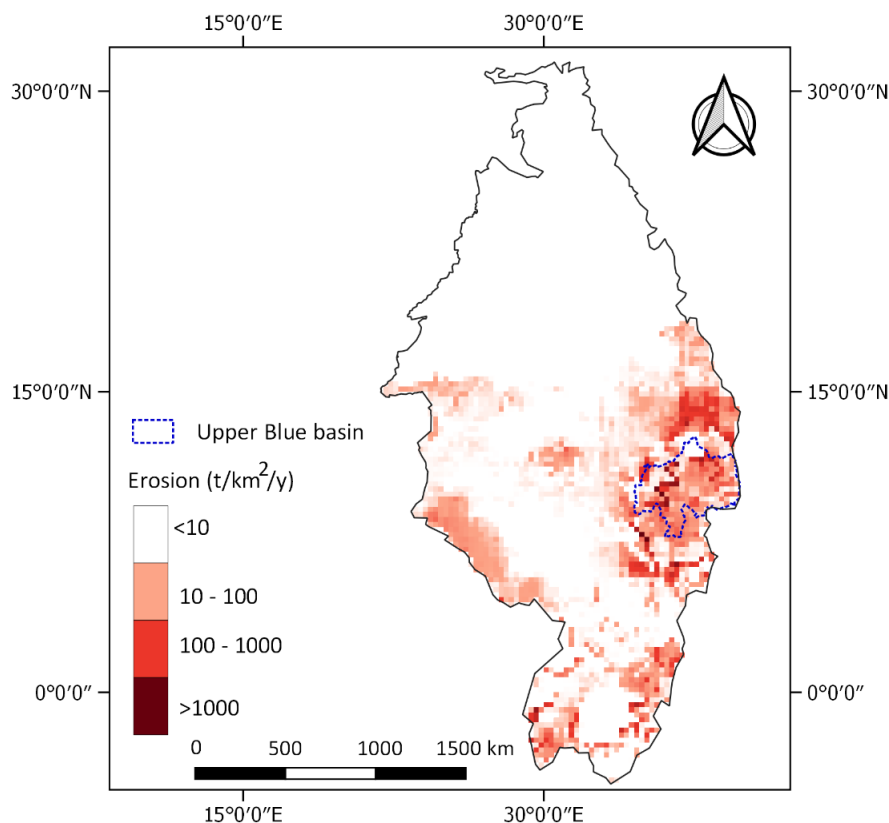
285 **Figure 8:** Change in erosion estimates (revised SWAT+ model minus default SWAT+ model); (a) absolute differences, (b) percentage differences



290 However, in some isolated regions, the revised SWAT+ model simulated an increase in soil erosion estimates as compared to the default model. In most of those regions, the global phenology data captures the irrigated cropping season which is often occurring in the dry seasons(Figure A2(c) and Figure A3(a)) which causes discrepancies by not representing the major growing season in the rainy season. This is attributed to the fact the global phenology data provides a single cropping season per pixel per year.

295 In order to validate the regional soil erosion estimates, the simulated soil loss from the revised SWAT+ model was compared with the spatial patterns in erosion rates from the literature. From published literature, Ethiopia is the one of the most documented countries in Northeast Africa with marginal information existing for other countries (Molina, 2009). The revised SWAT+ model shows that the regional soil erosion extent varies from zero to over 20500 t km⁻² y⁻¹, (Figure 9), revealing the severity of soil erosion in the Blue Nile basin (Ethiopian highlands) as compared to the other parts of the region.

300 Comparing with estimates from the Upper Blue Nile basin, the model estimated an erosion yield extent from 0 to 13000 t km⁻² y⁻¹ and a mean of 701 t km⁻² y⁻¹ which is slightly lower but comparable to a net soil erosion mean of 734 t km⁻² y⁻¹ reported by Haregeweyn et al., (2017) and soil erosion yield extents from zero to over 15000 t km⁻² y⁻¹ reported by Hurni, (1985), Betrie et al., (2011) and Haregeweyn et al., (2017). Tamene and Le, (2015) reported a net soil loss of 8500 t km⁻² y⁻¹ and 600 t km⁻² y⁻¹ in the Blue Nile and White Nile basins respectively. These estimates should be considered as indicative as comparing these values with the Northeast African regional model estimates can be challenging mainly due to the differences in the sizes of areas involved resulting from the different delineation procedures.



305 **Figure 9:** Spatial distribution of predicted annual average soil erosion at HRU level in Northeast Africa (2009 – 2015)

Even though the regional model underestimates the soil erosion in comparison with these localized studies, the order of magnitude is within the same range. The underestimation can be attributed to the finer resolution of datasets utilized by the local studies as compared to the coarse datasets utilized in the regional model. For example, Molnár and Julien, (1998) calculated soil erosion using different DEM grid sizes and concluded that the estimated slope gradients decreased as the cell size increased which influenced the topographic factor (LS) estimation. Additionally, the input global weather data is at a scale of 0.5° which makes it too coarse to capture the spatial variability of weather at a finer scale. This has been a challenge for large scale hydrological modelling (Chawanda et al., 2020), that needs to be addressed for better performance.

310 With that background, it is not wise to entirely consider the soil erosion estimates in this study as exact quantification but rather as close approximations. It is worth noting that the focus of this study was not soil erosion estimation but to illustrate a concept.

315

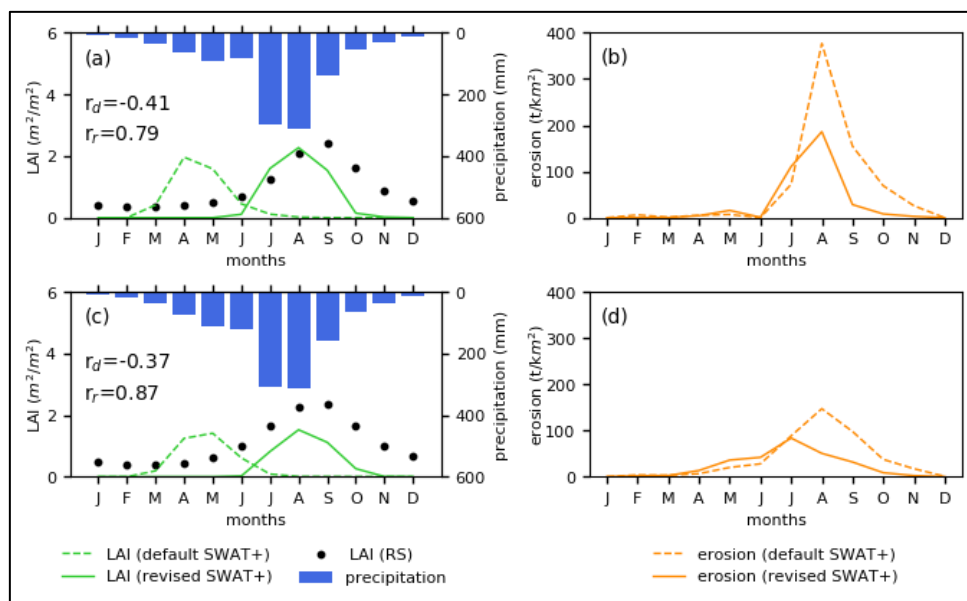
4. Conclusion

In this work, an approach has been developed for an improved representation of crop phenology and management in a regional SWAT+ model using decision tables and global datasets. In addition, global remote sensing datasets of LAI and ET have been

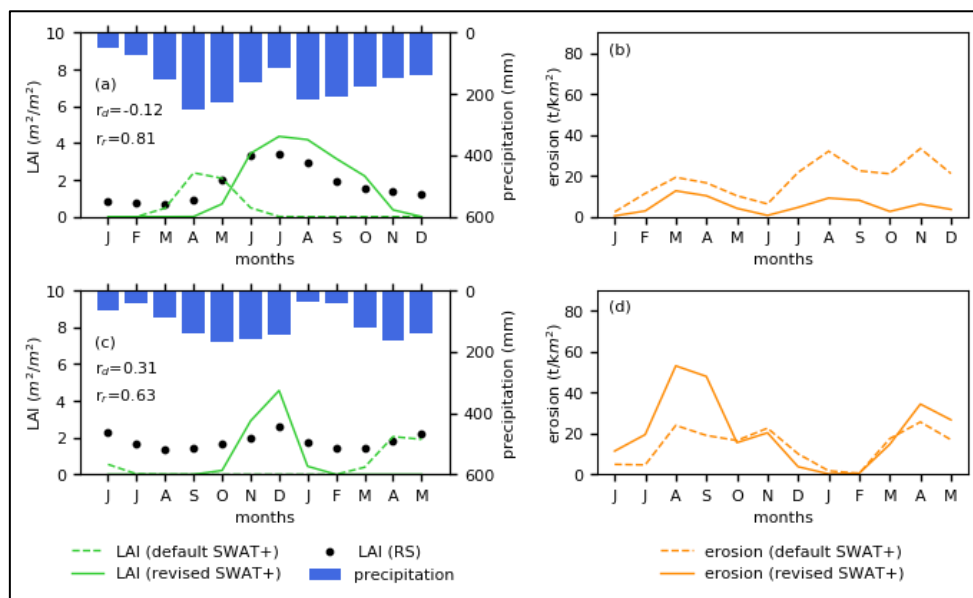


used for model evaluation. A comparison of the simulated LAI revealed improved temporal growth patterns in agreement with
 320 remote sensing LAI, especially for regions with a single cropping cycle. However, for regions with multiple cropping cycles,
 only one cropping cycle was represented as most global phenology datasets provide a single cropping cycle per year.
 The improvements in the SWAT+ model reduced the agricultural ET deficit by 50 % in comparison with the WaPOR ET,
 showing a strong linkage between hydrological response and agricultural land use representation. Additionally, this
 improvement in ET estimates is expected to reduce any calibration efforts needed to obtain the maximum possible ET as the
 325 physical process representation of crops is improved. A considerable reduction of 16 % in the average regional soil erosion
 estimates was noticed after implementing this approach. This impact on soil erosion estimates shows the importance of proper
 representation of crop processes and an important element for minimizing errors in soil erosion estimates.
 There is a need for global phenology datasets with multiple cropping seasons for further improvements in the crop
 representation, especially for improving crop processes in irrigated areas or areas with multiple rainy seasons. The approach
 330 developed in this research lays a foundation for improved agricultural land use representation with associated management
 practices at regional and global scales which will further improve regional to large scale hydrological and water quality impact
 assessments of global change.

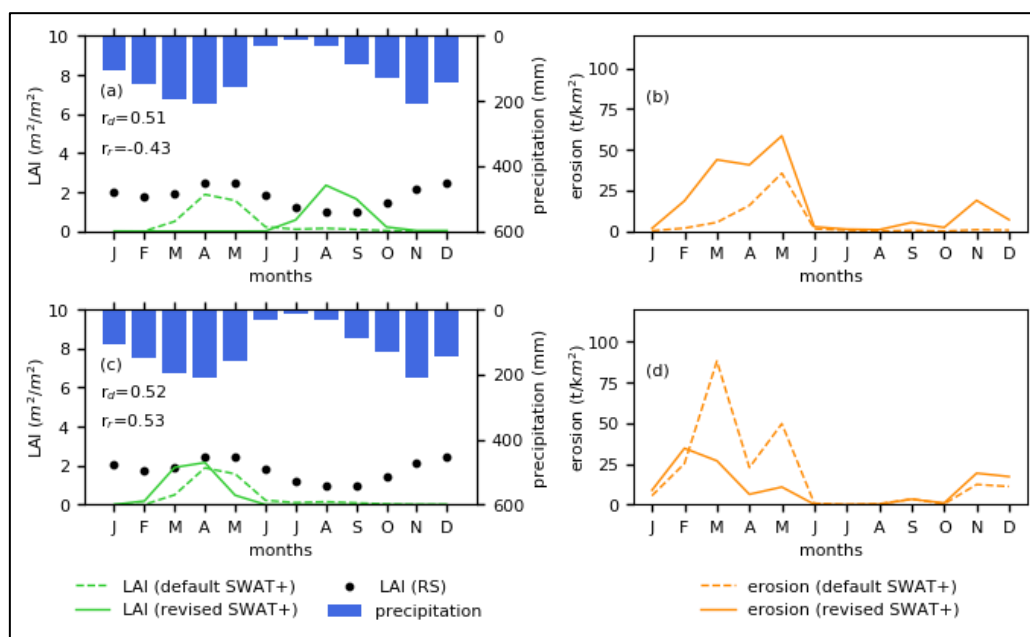
Appendix A



335 **Figure A1:** (a) LAI comparison for rainfed wheat, (b) Erosion estimates for rainfed wheat, (c) LAI comparison for irrigated wheat (d) Erosion estimates for irrigated wheat; in the Upper Blue Nile basin. The LAI correlation coefficients (r_d for the default SWAT+ model and r_r for the revised SWAT+ model)



340 **Figure A2:** (a) LAI comparison for irrigated maize – case1, (b) Erosion estimates for irrigated maize – case1, (c) LAI comparison for irrigated maize – case2 (d) Erosion estimates for irrigated maize – case2; in the Victoria basin. The LAI correlation coefficients (r_d for the default SWAT+ model and r_r for the revised SWAT+ model)



345 **Figure A3:** (a) LAI comparison for irrigated soy - case1, (b) Erosion estimates for irrigated soy - case1, (c) LAI comparison for irrigated soy - case2 (d) Erosion estimates for irrigated soy - case2; in the Victoria basin. The LAI correlation coefficients (r_d for the default SWAT+ model and r_r for the revised SWAT+ model)

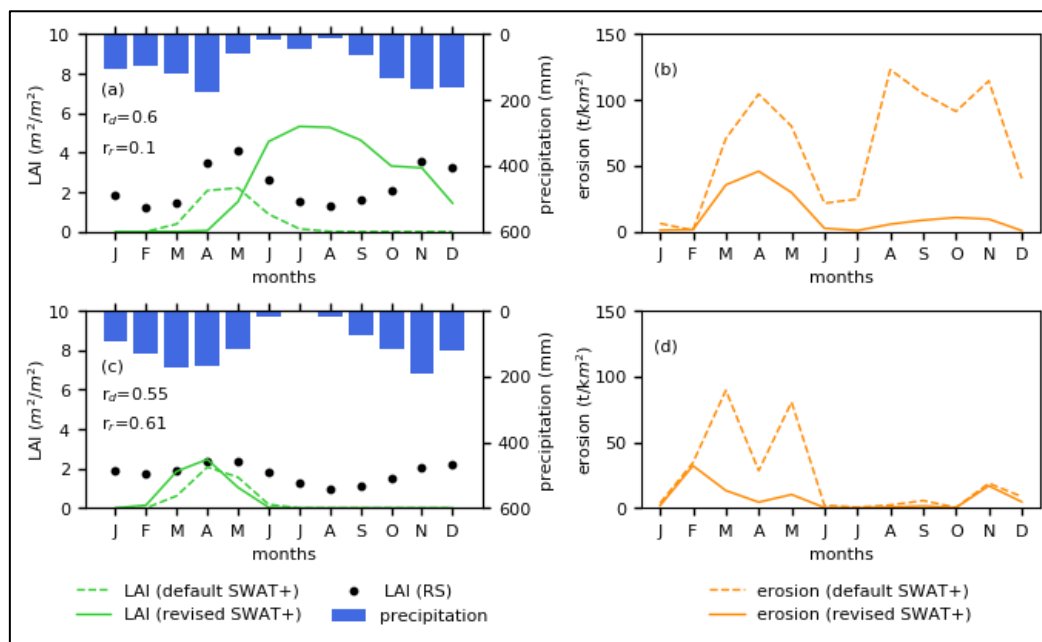


Figure A4: (a) LAI comparison for rainfed maize, (b) Erosion estimates for rainfed maize, (c) LAI comparison for rainfed soy (d) Erosion estimates for rainfed soy; in the Victoria basin. The LAI correlation coefficients (r_d for the default SWAT+ model and r_r for the revised SWAT+ model)

350 **Code availability:** This approach was created using python scripts available on the VUB-HYDR repository (https://github.com/VUB-HYDR/2021_Nkwasa_et_al). The revisions of the scripts are managed there and are available on request.

Author contributions: AN and AG designed this study. JJ provided the phenology datasets. CJC and AN set up the model. AN performed the model simulations, primary analysis and drafted the paper. All authors contributed to results interpretation and reviewed the paper.

Competing Interests: The authors declare that they have no conflict of interest.

Acknowledgement: The authors thank the Research Foundation – Flanders (FWO) for funding the International Coordination Action (ICA) “Open Water Network: Open Data and Software tools for water resources management” (project code G0E2621N) and the Flemish Research Council (VLIR) for funding the JOINT project “Global Open Water Academic Network: Joint Research and Education on Open Source Software for Integrated Water Resources Management” (project code T2019JOI022A105).

References

Abaci, O. and Papanicolaou, A. T.: Long-term effects of management practices on water-driven soil erosion in an intense agricultural sub-watershed: Monitoring and modelling, *Hydrol. Process. Int. J.*, 23, 2818–2837, 2009.



- 365 Alemayehu, T., van Griensven, A., and Bauwens, W.: Evaluating CFSR and WATCH Data as Input to SWAT for the Estimation of the Potential Evapotranspiration in a Data-Scarce Eastern-African Catchment, *J. Hydrol. Eng.*, 21, 05015028, [https://doi.org/10.1061/\(ASCE\)HE.1943-5584.0001305](https://doi.org/10.1061/(ASCE)HE.1943-5584.0001305), 2016.
- Alemayehu, T., van Griensven, A., Woldegiorgis, B. T., and Bauwens, W.: An improved SWAT vegetation growth module and its evaluation for four tropical ecosystems, *Hydrol. Earth Syst. Sci.*, 21, 4449–4467, <https://doi.org/doi:10.5194/hess-21-4449-2017>, 2017.
- 370
- Arnold, J., Bieger, K., White, M., Srinivasan, R., Dunbar, J., and Allen, P.: Use of decision tables to simulate management in SWAT+, *Water*, 10, 713, 2018.
- Arnold, J. G., Srinivasan, R., Muttiah, R. S., and Williams, J. R.: Large Area Hydrologic Modeling and Assessment Part I: Model Development1, *JAWRA J. Am. Water Resour. Assoc.*, 34, 73–89, <https://doi.org/doi:10.1111/j.1752-1688.1998.tb05961.x>, 1998.
- 375
- Arnold, J. G., Moriasi, D. N., Gassman, P. W., Abbaspour, K. C., White, M. J., Srinivasan, R., Santhi, C., Harmel, R. D., Van Griensven, A., and Van Liew, M. W.: SWAT: Model use, calibration, and validation, *Trans. ASABE*, 55, 1491–1508, 2012.
- Bégué, A., Arvor, D., Bellon, B., Betbeder, J., De Abelleira, D., P. D. Ferraz, R., Lebourgeois, V., Lelong, C., Simões, M., and R. Verón, S.: Remote Sensing and Cropping Practices: A Review, *Remote Sens.*, 10, 99, <https://doi.org/10.3390/rs10010099>, 2018.
- 380
- Betrie, G. D., Mohamed, Y. A., van Griensven, A., and Srinivasan, R.: Sediment management modelling in the Blue Nile Basin using SWAT model, *Hydrol. Earth Syst. Sci.*, 15, 807–818, <https://doi.org/10.5194/hess-15-807-2011>, 2011.
- Bieger, K., Arnold, J. G., Rathjens, H., White, M. J., Bosch, D. D., Allen, P. M., Volk, M., and Srinivasan, R.: Introduction to SWAT+, A Completely Restructured Version of the Soil and Water Assessment Tool, *JAWRA J. Am. Water Resour. Assoc.*, 53, 115–130, <https://doi.org/doi:10.1111/1752-1688.12482>, 2017.
- 385
- Biondi, D., Freni, G., Iacobellis, V., Mascaro, G., and Montanari, A.: Validation of hydrological models: Conceptual basis, methodological approaches and a proposal for a code of practice, *Phys. Chem. Earth Parts ABC*, 42–44, 70–76, <https://doi.org/10.1016/j.pce.2011.07.037>, 2012.
- Camberlin, P.: Nile Basin Climates, in: *The Nile: Origin, Environments, Limnology and Human Use*, edited by: Dumont, H. J., Springer Netherlands, Dordrecht, 307–333, https://doi.org/10.1007/978-1-4020-9726-3_16, 2009.
- 390
- Chawanda, C. J., Arnold, J., Thiery, W., and Griensven, A. van: Mass balance calibration and reservoir representations for large-scale hydrological impact studies using SWAT+, *Clim. Change*, 1–21, <https://doi.org/10.1007/s10584-020-02924-x>, 2020.
- Chen, F. and Xie, Z.: Effects of crop growth and development on regional climate: a case study over East Asian monsoon area, *Clim. Dyn.*, 38, 2291–2305, <https://doi.org/10.1007/s00382-011-1125-y>, 2012.
- 395
- Estel, S., Kuemmerle, T., Levers, C., Baumann, M., and Hostert, P.: Mapping cropland-use intensity across Europe using MODIS NDVI time series, *Environ. Res. Lett.*, 11, 024015, <https://doi.org/10.1088/1748-9326/11/2/024015>, 2016.
- FAO: Using remote sensing in support of solutions to reduce agricultural water productivity gaps, Rome, Italy, 2018.
- Farr, T. G., Rosen, P. A., Caro, E., Crippen, R., Duren, R., Hensley, S., Kobrick, M., Paller, M., Rodriguez, E., and Roth, L.: The shuttle radar topography mission, *Rev. Geophys.*, 45, 2007.
- 400



- 405 Fisher, J. B., Melton, F., Middleton, E., Hain, C., Anderson, M., Allen, R., McCabe, M. F., Hook, S., Baldocchi, D., Townsend, P. A., Kilic, A., Tu, K., Miralles, D. D., Perret, J., Lagouarde, J.-P., Waliser, D., Purdy, A. J., French, A., Schimel, D., Famiglietti, J. S., Stephens, G., and Wood, E. F.: The future of evapotranspiration: Global requirements for ecosystem functioning, carbon and climate feedbacks, agricultural management, and water resources, *Water Resour. Res.*, 53, 2618–2626, <https://doi.org/10.1002/2016WR020175>, 2017.
- Gong, T. T., Lei, H. M., Yang, D. W., Jiao, Y., and Yang, H. B.: Effects of vegetation change on evapotranspiration in a semiarid shrubland of the Loess Plateau, China., *Hydrol. Earth Syst. Sci. Discuss.*, 11, 2014.
- Ha, L. T., Bastiaanssen, W. G. M., Van Griensven, A., Van Dijk, A. I. J. M., and Senay, G. B.: Calibration of Spatially Distributed Hydrological Processes and Model Parameters in SWAT Using Remote Sensing Data and an Auto-Calibration Procedure: A Case Study in a Vietnamese River Basin, *Water*, 10, 212, <https://doi.org/10.3390/w10020212>, 2018.
- 410 Haregeweyn, N., Tsunekawa, A., Poesen, J., Tsubo, M., Meshesha, D. T., Fenta, A. A., Nyssen, J., and Adgo, E.: Comprehensive assessment of soil erosion risk for better land use planning in river basins: Case study of the Upper Blue Nile River, *Sci. Total Environ.*, 574, 95–108, <https://doi.org/10.1016/j.scitotenv.2016.09.019>, 2017.
- Hengl, T., Heuvelink, G. B. M., Kempen, B., Leenaars, J. G. B., Walsh, M. G., Shepherd, K. D., Sila, A., MacMillan, R. A., 415 Jesus, J. M. de, Tamene, L., and Tondoh, J. E.: Mapping Soil Properties of Africa at 250 m Resolution: Random Forests Significantly Improve Current Predictions, *PLOS ONE*, 10, e0125814, <https://doi.org/10.1371/journal.pone.0125814>, 2015.
- Hurni, H.: Erosion-productivity-conservation systems in Ethiopia, 1985.
- Hurt, G. C., Chini, L., Sahajpal, R., Frohling, S., Bodirsky, B. L., Calvin, K., Doelman, J. C., Fisk, J., Fujimori, S., Goldewijk, K. K., Hasegawa, T., Havlik, P., Heinemann, A., Humpenöder, F., Jungclaus, J., Kaplan, J., Kennedy, J., Kristzin, T., Lawrence, D., Lawrence, P., Ma, L., Mertz, O., Pongratz, J., Popp, A., Poulter, B., Riahi, K., Shevliakova, E., Stehfest, E., Thornton, P., Tubiello, F. N., van Vuuren, D. P., and Zhang, X.: Harmonization of Global Land-Use Change and Management for the Period 850–2100 (LUH2) for CMIP6, *Geosci. Model Dev. Discuss.*, 1–65, <https://doi.org/10.5194/gmd-2019-360>, 2020.
- 420 Iizumi, T., Kim, W., and Nishimori, M.: Modeling the Global Sowing and Harvesting Windows of Major Crops Around the Year 2000, *J. Adv. Model. Earth Syst.*, 11, 99–112, <https://doi.org/10.1029/2018MS001477>, 2019.
- 425 Jägermeyr et al.: Climate change signal in global agriculture emerges earlier in new generation of climate and crop models, *Nat. Food*, in revision.
- Lange, S.: Earth2Observe, WFDEI and ERA-Interim data Merged and Bias-corrected for ISIMIP (EWEMBI), <https://doi.org/10.5880/PIK.2016.004>, 2016.
- Leff, B., Ramankutty, N., and Foley, J. A.: Geographic distribution of major crops across the world, *Glob. Biogeochem. Cycles*, 18, <https://doi.org/10.1029/2003GB002108>, 2004.
- 430 Li, L., Friedl, M. A., Xin, Q., Gray, J., Pan, Y., and Frohling, S.: Mapping Crop Cycles in China Using MODIS-EVI Time Series, *Remote Sens.*, 6, 2473–2493, <https://doi.org/10.3390/rs6032473>, 2014.
- Lin, J., Zhang, J., Gu, Z., Chen, J., and Lyu, H.: A new approach of assessing soil erosion using the remotely sensed leaf area index and its application in the hilly area, *Yegetos- Int. J. Plant Res.*, 27, 1–12, 2014.
- 435 Lokupitiya, E., Denning, S., Paustian, K., Baker, I., Schaefer, K., Verma, S. B., Meyers, T., Bernacchi, C. J., Suyker, A. E., and Fischer, M. L.: Incorporation of crop phenology in Simple Biosphere Model (SiBcrop) to improve land-atmosphere carbon exchanges from croplands, 2009.



- Lotsch, A., Friedl, M. A., Anderson, B. T., and Tucker, C. J.: Coupled vegetation-precipitation variability observed from satellite and climate records, *Geophys. Res. Lett.*, 30, <https://doi.org/10.1029/2003GL017506>, 2003.
- 440 Lu, C. and Tian, H.: Global nitrogen and phosphorus fertilizer use for agriculture production in the past half century: shifted hot spots and nutrient imbalance, *Earth Syst. Sci. Data*, 9, 181–192, <https://doi.org/10.5194/essd-9-181-2017>, 2017.
- M. El-Marsafawy, S., Swelam, A., and Ghanem, A.: Evolution of Crop Water Productivity in the Nile Delta over Three Decades (1985–2015), *Water*, 10, 1168, <https://doi.org/10.3390/w10091168>, 2018.
- 445 Makowski, D., Nesme, T., Papy, F., and Doré, T.: Global agronomy, a new field of research. A review, *Agron. Sustain. Dev.*, 34, 293–307, <https://doi.org/10.1007/s13593-013-0179-0>, 2014.
- Molina, A.: Report on Soil Erosion Processes in the Nile basin, http://www.unesco.org/new/fileadmin/MULTIMEDIA/FIELD/Cairo/pdf/Report_on_soil_erosion_processes_in_the_Nile_Basin_1-Full_with_annex.pdf, 2009.
- 450 Molnár, D. K. and Julien, P. Y.: Estimation of upland erosion using GIS, *Comput. Geosci.*, 24, 183–192, [https://doi.org/10.1016/S0098-3004\(97\)00100-3](https://doi.org/10.1016/S0098-3004(97)00100-3), 1998.
- Monteith, J. L.: Radiation and crops, *Exp. Agric.*, 1, 241–251, 1965.
- Msigwa, A., Komakech, H. C., Verbeiren, B., Salvadore, E., Hessels, T., Weerasinghe, I., and Griensven, A. van: Accounting for Seasonal Land Use Dynamics to Improve Estimation of Agricultural Irrigation Water Withdrawals, *Water*, 11, 2471, <https://doi.org/10.3390/w11122471>, 2019.
- 455 Mueller, B., Seneviratne, S. I., Jimenez, C., Corti, T., Hirschi, M., Balsamo, G., Ciais, P., Dirmeyer, P., Fisher, J. B., Guo, Z., Jung, M., Maignan, F., McCabe, M. F., Reichle, R., Reichstein, M., Rodell, M., Sheffield, J., Teuling, A. J., Wang, K., Wood, E. F., and Zhang, Y.: Evaluation of global observations-based evapotranspiration datasets and IPCC AR4 simulations, *Geophys. Res. Lett.*, 38, <https://doi.org/10.1029/2010GL046230>, 2011.
- 460 Neitsch, S. L., Arnold, J. G., Kiniry, J. R., Williams, J. R., and King, K. W.: SWAT theoretical documentation, *Soil Water Res. Lab. Grassl.*, 494, 234–235, 2005.
- Neitsch, S. L., Arnold, J. G., Kiniry, J. R., and Williams, J. R.: Soil and water assessment tool theoretical documentation version 2009, Texas Water Resources Institute, 2011.
- 465 Nkwasa, A., Chawanda, C. J., Msigwa, A., Komakech, H. C., Verbeiren, B., and van Griensven, A.: How Can We Represent Seasonal Land Use Dynamics in SWAT and SWAT+ Models for African Cultivated Catchments?, *Water*, 12, 1541, <https://doi.org/10.3390/w12061541>, 2020.
- O’Neal, M. R., Nearing, M. A., Vining, R. C., Southworth, J., and Pfeifer, R. A.: Climate change impacts on soil erosion in Midwest United States with changes in crop management, *Catena*, 61, 165–184, 2005.
- Portmann, F. T., Siebert, S., and Döll, P.: MIRCA2000—Global monthly irrigated and rainfed crop areas around the year 2000: A new high-resolution data set for agricultural and hydrological modeling, *Glob. Biogeochem. Cycles*, 24, <https://doi.org/10.1029/2008GB003435>, 2010.
- Potter, P., Ramankutty, N., Bennett, E. M., and Donner, S. D.: Characterizing the spatial patterns of global fertilizer application and manure production, *Earth Interact.*, 14, 1–22, 2010.



- Schuol, J. and Abbaspour, K. C.: Calibration and uncertainty issues of a hydrological model (SWAT) applied to West Africa, *Adv. Geosci.*, 9, 137–143, 2006.
- 475 Schuol, J., Abbaspour, K. C., Yang, H., Srinivasan, R., and Zehnder, A. J. B.: Modeling blue and green water availability in Africa, *Water Resour. Res.*, 44, <https://doi.org/10.1029/2007WR006609>, 2008.
- Siebert, S., Henrich, V., Frenken, K., and Burke, J.: Global map of irrigation areas version 5, *Rheinische Friedrich-Wilhelms- Univ. Bonn Ger. Agric. Organ. U. N. Rome Italy*, 2, 1299–1327, 2013.
- 480 Sood, A. and Smakhtin, V.: Global hydrological models: a review, *Hydrol. Sci. J.*, 60, 549–565, <https://doi.org/10.1080/02626667.2014.950580>, 2015.
- Souza, V. F. C. de, Bertol, I., and Wolschick, N. H.: Effects of soil management practices on water erosion under natural rainfall conditions on a Humic Dystrudept, *Rev. Bras. Ciênc. Solo*, 41, 2017.
- Srinivasan, R., Zhang, X., and Arnold, J.: SWAT ungauged: hydrological budget and crop yield predictions in the Upper Mississippi River Basin, *Trans. ASABE*, 53, 1533–1546, 2010.
- 485 Srivastava, A., Kumari, N., and Maza, M.: Hydrological Response to Agricultural Land Use Heterogeneity Using Variable Infiltration Capacity Model, *Water Resour. Manag.*, 34, 3779–3794, <https://doi.org/10.1007/s11269-020-02630-4>, 2020.
- Sugita, M., Matsuno, A., El-Kilani, R. M. M., Abdel-Fattah, A., and Mahmoud, M. A.: Crop evapotranspiration in the Nile Delta under different irrigation methods, *Hydrol. Sci. J.*, 62, 1618–1635, <https://doi.org/10.1080/02626667.2017.1341631>, 2017.
- 490 Sundborg, A. and White, W. R.: Sedimentation problems in river basins, France, 1982.
- Swain, A.: Challenges for water sharing in the Nile basin: changing geo-politics and changing climate, *Hydrol. Sci. J.*, 56, 687–702, <https://doi.org/10.1080/02626667.2011.577037>, 2011.
- Tamene, L. and Le, Q. B.: Estimating soil erosion in sub-Saharan Africa based on landscape similarity mapping and using the revised universal soil loss equation (RUSLE), *Nutr. Cycl. Agroecosystems*, 102, 17–31, <https://doi.org/10.1007/s10705-015-9674-9>, 2015.
- 495 Twine, T. E., Kucharik, C. J., and Foley, J. A.: Effects of Land Cover Change on the Energy and Water Balance of the Mississippi River Basin, *J. Hydrometeorol.*, 5, 640–655, [https://doi.org/10.1175/1525-7541\(2004\)005<0640:EOLCCO>2.0.CO;2](https://doi.org/10.1175/1525-7541(2004)005<0640:EOLCCO>2.0.CO;2), 2004.
- 500 Waha, K., Müller, C., Bondeau, A., Dietrich, J. P., Kurukulasuriya, P., Heinke, J., and Lotze-Campen, H.: Adaptation to climate change through the choice of cropping system and sowing date in sub-Saharan Africa, *Glob. Environ. Change*, 23, 130–143, <https://doi.org/10.1016/j.gloenvcha.2012.11.001>, 2013.
- Williams, J. R. and Berndt, H. D.: Sediment yield prediction based on watershed hydrology, *Trans. ASAE*, 20, 1100–1104, 1977.
- 505 Williams, J. R. and Singh, V.: The EPIC Model, Computer models of watershed hydrology, *Water Resour. Publ. Highl. Ranch Colo.*, 909–1000, 1995.



Xiong, J., Thenkabail, P. S., Gumma, M. K., Teluguntla, P., Poehnelt, J., Congalton, R. G., Yadav, K., and Thau, D.: Automated cropland mapping of continental Africa using Google Earth Engine cloud computing, *ISPRS J. Photogramm. Remote Sens.*, 126, 225–244, <https://doi.org/10.1016/j.isprsjprs.2017.01.019>, 2017.

510 Yin, X. and Struik, P. C.: C3 and C4 photosynthesis models: An overview from the perspective of crop modelling, *NJAS - Wagening. J. Life Sci.*, 57, 27–38, <https://doi.org/10.1016/j.njas.2009.07.001>, 2009.

Zhang, X., Friedl, M. A., Schaaf, C. B., Strahler, A. H., and Liu, Z.: Monitoring the response of vegetation phenology to precipitation in Africa by coupling MODIS and TRMM instruments, *J. Geophys. Res. Atmospheres*, 110, <https://doi.org/doi:10.1029/2004JD005263>, 2005.